https://doi.org/10.5194/egusphere-2023-945
Preprint. Discussion started: 31 May 2023

A robust error correction method for numerical weather prediction wind speed based on Bayesian optimization, Variational Mode Decomposition, Principal Component Analysis, and Random Forest: VMD-PCA-RF (version 1.0.0)

Shaohui Zhou[1], Chloe Yuchao Gao[2*], Zexia Duan[1], Xingya Xi[3], and Yubin Li[1]

[1]Collaborative Innovation Centre on Forecast and Evaluation of Meteorological Disasters, Key Laboratory for Aerosol-Cloud-Precipitation of China Meteorological Administration, School of Atmospheric Physics, Nanjing University of Information Science and Technology, Nanjing, 210044, China.

[2]Department of Atmospheric and Oceanic Sciences and Institute of Atmospheric Sciences, Fudan University, Shanghai, 200438, China.

[3]School of Atmospheric Sciences, Sun Yat-sen University, and Southern Marine Science and Engineering Guangdong Laboratory (Zhuhai), Zhuhai, 519082, China

Correspondence to: gyc@fudan.edu.cn

Abstract. Accurate wind speed prediction is crucial for the safe utilization of wind resources. However, current single-value deterministic numerical weather prediction methods employed by wind farms do not adequately meet the actual needs of power grid dispatching. In this study, we propose a new hybrid forecasting method for correcting 10-meter wind speed predictions made by the Weather Research and Forecasting (WRF) model. Our approach incorporates Variational Mode Decomposition (VMD), Principal Component Analysis (PCA), and five artificial intelligence algorithms: Deep Belief Network (DBN), Multilayer Perceptron (MLP), Random Forest (RF), eXtreme Gradient Boosting (XGBoost), light Gradient Boosting Machine (lightGBM), and the Bayesian Optimization Algorithm (BOA). We first construct WRF-predicted wind speeds using the Global Prediction System (GFS) model output based on prediction results. We then perform two sets of experiments with different input factors and apply BOA optimization to debug the four artificial intelligence models, ultimately building the final models. Furthermore, we compare the forementioned five optimal artificial intelligence models suitable for five provinces in southern China in the wintertime: VMD-PCA-RF in December 2021 and VMD-PCA-lightGBM in January 2022. We find that the VMD-PCA-RF evaluation indexes exhibit relative stability over nearly a year: correlation coefficient (R) is above 0.6, accuracy rate (FA) is above 85 %, mean absolute error (MAE) is below 0.6 m/s, root mean square error (RMSE) is below 0.8 m/s,

https://doi.org/10.5194/egusphere-2023-945
Preprint. Discussion started: 31 May 2023

relative mean absolute error (rMAE) is below 60 %, and relative root mean square error (rRMSE) is below 75 %. Thus, for its promising performance and excellent year-round robustness, we recommend adopting the proposed VMD-PCA-RF method for improved wind speed prediction in models.

1 Introduction

Sustainable energy plays a vital role in reducing carbon footprint and increasing system reliability (Hanifi et al., 2020). As renewable energy sources have a negligible carbon footprint, they have become the preferred choice for many industries in the power sector (Dhiman and Deb, 2020). Among these sources, wind energy is a crucial low-carbon energy technology with the potential to become a sustainable energy source (Tascikaraoglu and Uzunoglu, 2014). In 2022, the global wind power capacity reached 906 GW, with a 9 % year-on-year increase due to a newly installed capacity of 77.6 GW. The global onshore wind market increased by 68.8 GW, while facing a 5 % growth decline compared to the previous year. Such change is attributed to a slowdown in China and the U.S., the world's two largest wind markets that account for over two-thirds of the world's onshore wind farm installations (Joyce and Feng, 2023). Therefore, accurate and stable wind speed prediction (WSP) is very important for the safe and stable operation of the power grid system and improving the utilization rate of wind energy and economic development (Guo et al., 2021; Xiong et al., 2022; Tang et al., 2021).

Current WSP algorithms are primarily categorized into physical algorithms (Zhao et al., 2016), statistical algorithms (Wang and Hu, 2015; Barthelmie et al., 1993), machine learning (ML) algorithms (Huang et al., 2019; Salcedo-Sanz et al., 2011; Ma et al., 2020), and hybrid algorithms (Deng et al., 2020; Xu et al., 2021; Zhao et al., 2019; Xiong et al., 2022; Tang et al., 2021). Physical methods, such as numerical weather prediction (NWP), are commonly used in wind speed forecasting. NWP, which accounts for atmospheric processes and physical laws, solves discrete mass, momentum, and energy conservation equations along with other fundamental physical principles, establishing itself as a widely adopted and reliable physical method. Currently, the High-resolution Limited Area Model (HIRLAM) (Landberg, 1999), the European Center for Medium-Range Weather Forecast (ECMWF) model, the fifth-generation mesoscale model (MM5) (Salcedo-Sanz et al., 2009), and the Weather Research and Forecasting Model (WRF) (Prósper et al., 2019) are extensively utilized for wind speed prediction.

https://doi.org/10.5194/egusphere-2023-945
Preprint. Discussion started: 31 May 2023

However, NWP modeling faces challenges due to the selection of parameterization schemes, such as model microphysics and systematic errors, which exhibit temporal and spatial differences and uncertainties. These uncertainties hinder the accuracy of NWP models in wind speed prediction, making it difficult to meet the rising demands of the grid system (Zhao et al., 2019; Xu et al., 2021).

Studies have demonstrated that enhancing the accuracy of numerical weather prediction (NWP) models and correcting prediction errors can effectively minimize the errors associated with wind speed prediction. These research endeavors have typically sought to optimize the physical and dynamic parameters of the NWP model (Cheng et al., 2013), refine the model structure (Jiménez and Dudhia, 2012), or improve the accuracy of model inputs through preprocessing and denoising techniques (Xu et al., 2015). Additionally, improving initial field error through methods, such as target observation and data assimilation (Williams et al., 2013), can also minimize wind speed errors predicted by NWP models.

Physical methods are generally more appropriate for long-term wind speed prediction, such as those 48-72 hours in advance, while their practical application in short-term forecasting is limited (Zhao et al., 2019; Deng et al., 2020; James et al., 2018). In contrast, statistical methods utilize historical data to establish a relationship between input and output variables and are therefore well-suited for short-term wind speed prediction. They are usually time series models, such as Autoregressive Moving Average (ARMA) (Erdem and Shi, 2011) and Autoregressive Integrated Moving Average (ARIMA) (Wang and Hu, 2015). Whereas filtering models (Cassola and Burlando, 2012; Chen and Yu, 2014), machine learning models (Hu et al., 2013), and hybrid models (Huang et al., 2019) have been gradually developed to further improve wind speed prediction accuracy.

With purely statistical models becoming less suitable for wind speed predictions beyond 6 hours, the use of a combination of physical and statistical methods has gained growing interest (Zjavka, 2015; Xu et al., 2021). The error correction model improves the accuracy of the NWP model by training the relationship between the NWP predictor variables and the observed correlation variables (Sun et al., 2019). However, traditional error prediction models rely solely on historical wind speed sequences as input factors (Deng et al., 2020; Guo et al., 2021) and do not incorporate the characteristic meteorological factors forecasted by the WRF model. Studies have shown that considering all relevant historical meteorological factors can lead to more accurate predictions compared to only taking into

https://doi.org/10.5194/egusphere-2023-945
Preprint. Discussion started: 31 May 2023

account historical wind speed (Zhang et al., 2019c). Therefore, it is crucial to include meteorological characteristic factors as input in the prediction model.

For an error prediction model, wind speed is the most important input factor. Traditionally, the error prediction model uses historical wind speed data as input, without any feature selection. Feature selection methods, such as filtering methods, are commonly used in time series analysis. Currently, empirical mode decomposition (EMD) (Liu et al., 2018; Guo et al., 2012), ensemble empirical mode decomposition (EEMD) (Wang et al., 2017), wavelet decomposition (WD) (Zhang et al., 2019b), variational mode decomposition (VMD) (Hu et al., 2021; Zhang et al., 2019a), and other filtering methods are used to select key features in the wind speed data. As mentioned above, studies have shown that these feature selection methods can effectively extract the hidden features in the wind speed series to improve wind speed prediction accuracy. However, despite the effectiveness of wind speed filtering methods in wind speed prediction, only a few studies have applied these methods to the correction of wind speed errors in NWP forecasting (Xu et al., 2021; Li et al., 2022).

In addition, traditional error correction methods generally adopt linear regression (Dong et al., 2013), multiple linear regression (Liu et al., 2016), machine learning (Salcedo-Sanz et al., 2011), and deep learning algorithms (Zhang et al., 2019c). However, the efficacy of machine learning and deep learning algorithms is highly dependent on the selection of model parameters (Guo et al., 2021; Xiong et al., 2022). The Bayesian optimization algorithm (Li and Shi, 2010; Guo et al., 2021) is considered a relatively advanced algorithm for optimizing model parameters and has been widely used in MATLAB and Python packages.

In this study, we investigate a multi-step wind speed forecasting model that combines NWP simulation and an error correction strategy. We present two sets of experiments divided into three steps: (1) we use the first group of experiments to extract hidden features from various meteorological elements forecasted by NWP; The second group of experiments mainly focuses on the wind speed forecast of NWP, and the VMD-PCA algorithm is used to extract the hidden features in the forecasted wind speed; each set of experimental input factors is matched with the actual 10-meter wind speed data of 410 stations in time and space; (2) we employ four advanced machine learning algorithms optimized by the BOA algorithm, and DBN deep learning algorithm to train the two groups of experiments and perform 5-fold cross-validation; and (3) we analyze six distinct wind speed error indicators to compare

https://doi.org/10.5194/egusphere-2023-945
Preprint. Discussion started: 31 May 2023

and identify the most suitable wind speed error correction schemes for the five southern provinces in winter and throughout most of the year. The remainder of this paper is organized into sections discussing the effects of the BOA-VMD-PCA approach, the interpretability of RF feature importance, and the stability analysis of the proposed models.

2 Data and methods

2.1 Data

The target observation data includes 2-m air temperature, 2-m specific humidity, 10-meter wind speed, surface pressure, and precipitation. These data are collected on equivalent latitude and longitude grid scale, primarily from five provinces in China: Guangdong, Guangxi, Yunnan, Guizhou, and Hainan, covering a geographical range of 15-32.97°N and 94-120.97°E. The spatial resolution of the grid is 0.03° × 0.03° and the temporal resolution is 1 hour. The dataset is constructed through the integration of multiple sources, including ground and satellite data, and is refined using advanced techniques such as multi-grid variational assimilation, physical inversion, and terrain correction. This dataset exhibits superior quality in comparison to other products, offering higher spatial and temporal resolutions. For the purposes of this paper, the 10-meter wind speed data is interpolated across 410 sites, as illustrated in Figure 1.

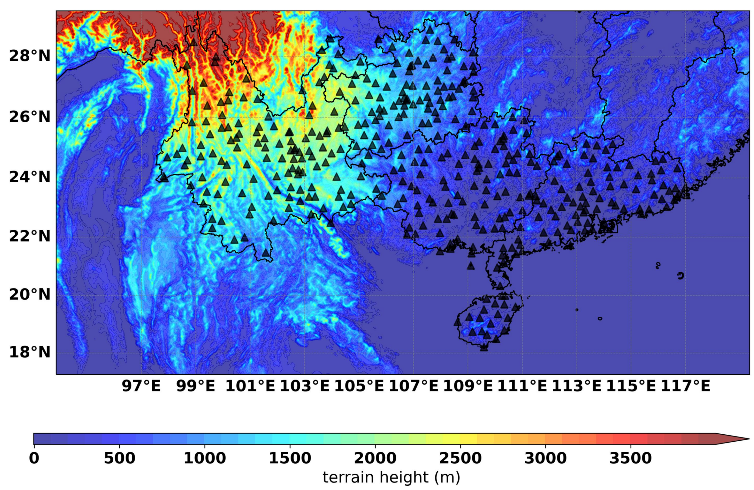

Figure 1: The elevation map of the five southern provinces in china (black triangles represent weather stations).

https://doi.org/10.5194/egusphere-2023-945
Preprint. Discussion started: 31 May 2023

2.2 Methods

2.2.1 WRF simulation

The WRF 4.2 model, developed by the United States' National Center for Environmental Prediction (NCEP), represents a new generation of mesoscale numerical models with numerous applications in research forecasting. The WRF model, written in Fortran 90 language, offers advantages such as portability, scalability, and high efficiency. It employs Arakawa C-grid points in the horizontal direction and terrain-following mass coordinates in the vertical direction. When forecasting meteorological elements, the WRF model uses the US Global Weather Forecast Data (GFS) developed by NCEP and the National Center for Atmospheric Research (NCAR). The GFS system includes data related to the atmosphere and land variables, such as temperature, precipitation, and wind data. The system is updated every 6 hours, at 0:00, 6:00, 12:00, and 18:00 UTC, and provides predictions for the subsequent eight days. Given that the time scale of the meteorological station data in the study area is 1 hour, the forecast data time interval of the WRF model is also set to 1 hour. As a widely used numerical weather forecast model, the WRF model is suitable for weather studies from a few meters to several thousand kilometers. Therefore, this paper uses the WRF model to predict 10-meter wind speed as the input factor for the error correction model (Xu et al., 2021).

Using the WRF model in combination with daily data resolution of 0.25° × 0.25°, the model initiates at 18:00 UTC and generates forecasts every 3 hours for a total duration of 102 hours. The regular Global Forecast System (GFS) forecast field data serve as the initial field and lateral boundary conditions for the WRF model. Surface static data, such as terrain, soil data, and vegetation coverage, are derived from the Moderate Resolution Imaging Spectroradiometer (MODIS) satellite with a resolution of 15 seconds (approximately 500 meters). Incorporating a two-layer grid nesting configuration, the forecast area is illustrated in Figure 2. The grid dimensions are 600×500 and 967×535, with horizontal grid resolutions of 9 km and 3 km, respectively. The grid center points are set at 29°N and 96°E. The "CONUS" parameterization scheme is used, including the Thompson microphysics scheme, the Tiedtke cumulus parameterization scheme, the RRTMG long-wave and short-wave radiation schemes, the Mellor-Yamada-Janjić (MYJ) boundary layer and near-surface parameterization schemes, and the MYJ surface layer parameterization scheme. The Noah Land

https://doi.org/10.5194/egusphere-2023-945
Preprint. Discussion started: 31 May 2023

Surface Model (LSM) is utilized for the surface process plan, generating a WRFOUT numerical weather forecast file including meteorological elements such as temperature, humidity, and precipitation. The WRF configuration process is detailed in Table 1.

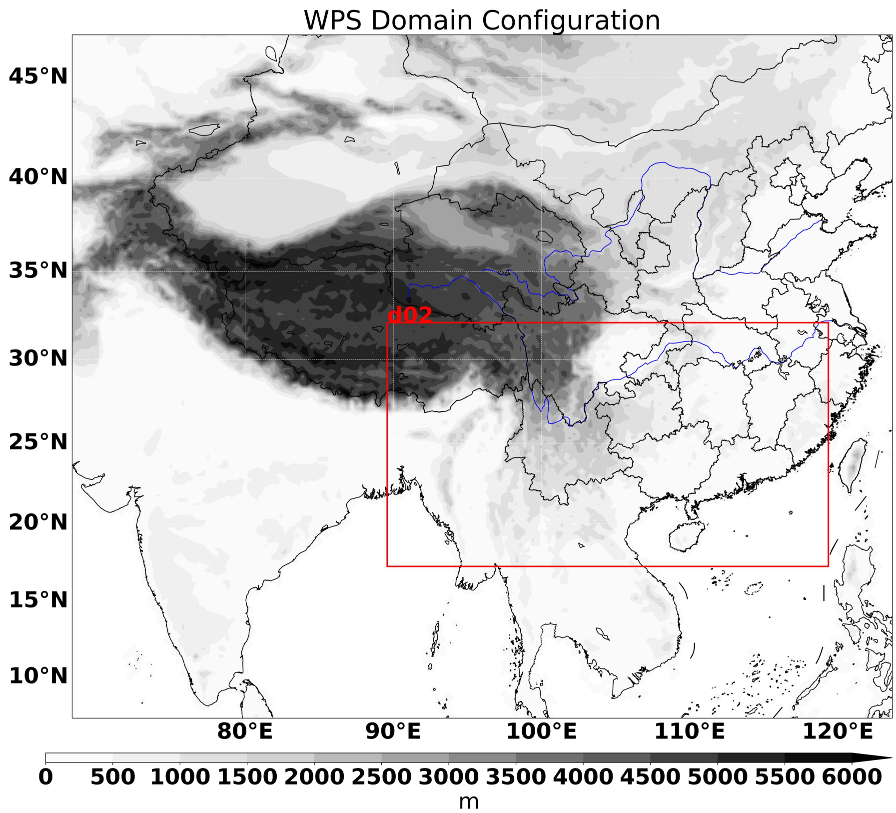

Figure 2: Schematic diagram of the simulation area of the WRF model.

Table 1: WRF configuration scheme

Model (Version)	WRF (V4.2)	
Domains	D1	D2
Horizontal grid points	600*500	967*535
Δx (km)	9	3
Vertical layers	58	
Longwave radiation	RRTMG (Iacono et al. 2008)	
Shortwave radiation	RRTMG (Iacono et al. 2008)	
Land surface	Noah LSM (Chen et al. 1997)	
Surface layer	MYJ (Janjic 1994)	
Microphysics	Thompson (Thompson et al. 2008)	

https://doi.org/10.5194/egusphere-2023-945
Preprint. Discussion started: 31 May 2023

Boundary layer	MYJ (Janjic 1994)
Cumulus	Tiedtke (Tiedtke 1989, Zhang et al. 2011)

2.2.2 Variational mode decomposition

As a new filtering method, VMD is robust in feature selection. The VMD algorithm decomposes a time series signal into several intrinsic mode functions (Isham et al., 2018). The sum of the modes equals the original signal, and the sum of the bandwidths is the smallest. The analysis signal is calculated using the Hilbert transform to estimate the modal bandwidth. The optimization model is described as

$$\left\{ \min_{\{u_k\},\{\omega_k\}} \left\{ \sum_{k=1}^{K} \left\| \partial_t \left[\left(\delta(t) + \frac{j}{\pi t} \right) u_k(t) \right] e^{-j\omega_k t} \right\|_2^2 \right\} s.t. \quad \sum_{k=1}^{K} u_k = v \right. \qquad (1.1)$$

where K is the total number of modes, u_k is the decomposed K-th mode, w_k is the corresponding center frequency, and v is the time-series signal, representing the wind speed sequence predicted by the WRF model in this study.

The above constrained problem can be transformed into an unconstrained problem using the Lagrangian function:

$$L(\{u_k\},\{\omega_k\},\lambda) = \omega_k^{n+1} = \frac{\int_0^\infty \omega \left|\hat{u}_k(\omega)\right|^2 d\omega}{\int_0^\infty \left|\hat{u}_k(\omega)\right|^2 d\omega} \sum_{k=1}^{K} \| \partial_t \left[\left(\delta(t) + \frac{j}{\pi t} \right) u_k(t) \right.$$

$$\left. \times \right] e^{-j\omega_k t} \|_2^2 + \| v(t) - \sum_{k=1}^{K} u_k(t) \|_2^2 + \left\langle \lambda(t), v(t) - \sum_{k=1}^{K} u_k(t) \right\rangle \qquad (1.2)$$

where α is the penalty parameter and $\lambda(t)$ is the Lagrange multiplier.

Then we update u_k, w_k, and λ using the alternating direction method of the multiplier:

$$\hat{u}_k^{n+1}(\omega) = \frac{\hat{v}(\omega) - \sum_{i \neq k} \hat{u}_i(\omega) + \frac{\hat{\lambda}(\omega)}{2}}{1 + 2\alpha\left(\omega - \omega_k\right)^2} \qquad (1.3)$$

$$\omega_k^{n+1} = \frac{\int_0^\infty \omega \left|\hat{u}_k(\omega)\right|^2 d\omega}{\int_0^\infty \left|\hat{u}_k(\omega)\right|^2 d\omega} \qquad (1.4)$$

$$\hat{\lambda}^{n+1}(\omega) = \hat{\lambda}^{n}(\omega) + \tau \left[\hat{v}(\omega) - \sum_{k=1}^{K} \hat{u}_k^{n+1}(\omega) \right] \qquad (1.5)$$

https://doi.org/10.5194/egusphere-2023-945
Preprint. Discussion started: 31 May 2023

where τ is the update parameter.

When the accuracy (left side of the following expression) meets the following condition, u_k, w_k and λ would stop updating:

$$\sum_{k=1}^{K} \frac{\| \hat{u}_k^{n+1} - \hat{u}_k^{n} \|_2^2}{\| \hat{u}_k^{n} \|_2^2} < \varepsilon \qquad (1.6)$$

where ε is the tolerance of the convergence criterion.

The VMD algorithm is implemented to decompose the wind speed signal predicted by the WRF model. When using multiple sub-signals instead of the original signal, more features of the wind speed can be obtained. Therefore, it is beneficial to improve the prediction accuracy when using the sub-signal as input to the error correction model (Xu et al., 2021; Li et al., 2022).

2.2.3 Principal Component Analysis

Subsequences obtained by VMD usually have several illusory components. Using PCA to extract the principal components of subsequences increases the number of features input to the model and reduces the dimension of the data decomposed by VMD. When pcs are used as the input of the error prediction algorithm, the pcs fully reflect the characteristics of the subsequence and reduce the model complexity. The pcs y_k, k=1, 2, …, K of the subsequence matrix U and the cumulative contribution rate η_n of first n principal components are expressed as:

$$y_k = c_k^{'} U \qquad (1.7)$$

$$\eta_n = \frac{\sum_{k=1}^{n} \lambda_k}{\sum_{k=1}^{K} \lambda_k} \qquad (1.8)$$

where c_k is the corresponding characteristic unit vector, with k=1, 2, …, K; λ_k is the characteristic root, with $\lambda_1 \geq \lambda_2 \geq \ldots \geq \lambda_K$.

2.2.4 Proposed hybrid forecasting algorithms

This study used five machine learning algorithms to conduct ten experiments across two main paths. The first path involves increasing the variables related to wind speed in the forecast field, while the second path entails extracting potential characteristic information of the forecast wind speed through VMD and PCA and reducing the characteristic quantity of other forecast data. The overarching

https://doi.org/10.5194/egusphere-2023-945
Preprint. Discussion started: 31 May 2023

goal is to achieve accurate correction of the forecast field wind speed. The flowchart of the artificial intelligence models used to correct the WRF predicted wind speed for the two main experimental paths is illustrated in Figure 3 and comprises the following three steps:

Step 1. Data fusion, cleaning, and standardization: As depicted in Figure 3, this paper proposes two distinct experimental paths, with the primary difference being the selection of input variables. In Experiment 1, as shown in Figure 6(c), 12 sets of data are selected from the WRF forecast field, including altitude, 10-meter wind speed, latitude, longitude, surface pressure, relative humidity, 10-meter meridional wind, 10-meter zonal wind, 2-meter temperature, 2-meter dew point temperature, 10-meter wind direction, and hourly precipitation. Experiment 2, as illustrated in Figure 6(d), derives 8 sets of data by reducing the selected WRF field forecast data, including altitude, 10-meter wind speed, latitude, longitude, surface pressure, relative humidity, 2-meter temperature, and hourly precipitation. The focus is on unearthing hidden characteristic information of forecast wind speed. In this experiment, the wind speed is decomposed into 9 Intrinsic Mode Functions (IMF) using VMD. Subsequently, a low-dimensional wind speed vector is extracted from the 9 IMF components via PCA dimensionality reduction, and all data are concatenated to construct the input factors for the model in Experiment 2. Missing and outlier values are removed from the dataset. The two experiments standardize 12 sets of meteorological elements (8 sets of meteorological elements in Figure 4, 9 IMF components, and three PCA vectors in Figure 5) and wind speed observation data, respectively. Standardization addresses the issue of varying meteorological factor values during training, which may result in different contributions. In this paper, the 24-hour forecast data correspond to the observation data of the subsequent 24 hours. The dataset spans from 00:00 on December 1, 2021, to 23:00 on February 28, 2022, totaling 2160 hours and encompassing 410 weather stations. Consequently, the original dataset comprises 2160*410 samples, with each sample containing 12 meteorological features in Experiment 1 and 20 input features in Experiment 2.

Step 2. BOA optimization of AI models and cross-validation: In this study, the dataset is partitioned into training, validation, and test sets in accordance with the time series. February 2022 serves as the training and validation sets, while December 2021 and January 2022 constitute the test set. The training and validation sets are divided based on five-fold cross-validation. Both experiments employ five machine learning algorithms (DBN, MLP, RF, XGBoost, and LightGBM) to construct

https://doi.org/10.5194/egusphere-2023-945
Preprint. Discussion started: 31 May 2023

distinct machine learning models. Concurrently, this paper utilizes the BOA algorithm to tune the parameters of all models, except for DBN, resulting in the optimal hyperparameters for each model.

Step 3. Model evaluation and error analysis: The trained machine learning models are applied to the test set to obtain the revised wind speed data, and ultimately, the accuracy of all models is assessed through the wind speed evaluation index. The ultimate goal here is to identify the best wind speed correction model suitable for the entire year. Accordingly, the generalization of all models is evaluated across other seasonal months of the year, culminating in the selection of the best model.

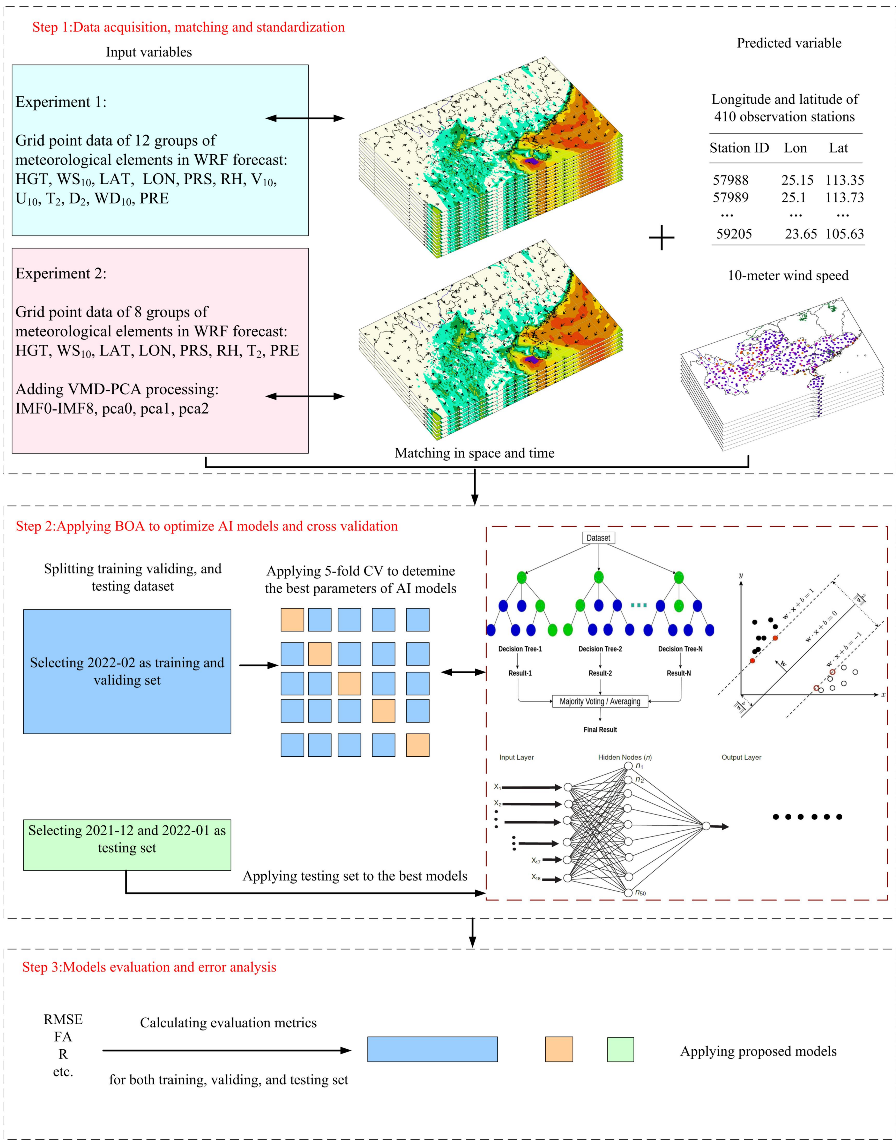

https://doi.org/10.5194/egusphere-2023-945
Preprint. Discussion started: 31 May 2023

Figure 3: Flowchart of the AI model used to correct WRF-predicted wind speeds in the two main experimental pathways.

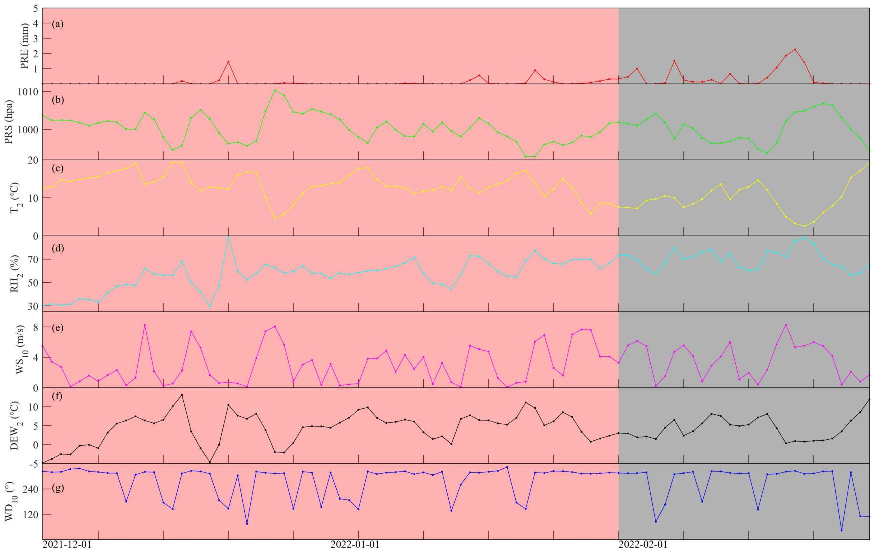

Figure 4: Daily average hourly rainfall (a), surface pressure (b), 2-meter temperature (c), 2-meter relative humidity (d), 10-meter wind speed (e), 2-meter dew point temperature (f), and 10-meter wind direction (g) which are located at Guangdong Lechang Station from December 1, 2021, to February 28, 2022. (February 2022 represents the training and verification sets, and December 2021 to January 2022 represents the testing set).

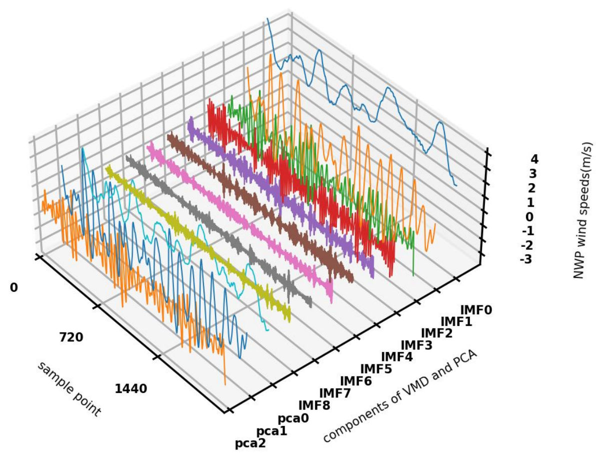

Figure 5: Three-dimensional view of 12 wind speed components after VMD and PCA processing of the 10-meter forecast wind speed at Lechang Station in Guangdong from December 1, 2021, to February 28, 2022.

2.2.5 Evaluation indicators

There are many commonly used predictive effect evaluation indicators. This article uses the following evaluation indicators: correlation coefficient (R), root mean square error (RMSE), mean absolute error (MAE), relative root mean square error (rRMSE), relative mean absolute error (rMAE), percentage of absolute error not greater than 1 m/s (FA). Six error indicators are used to evaluate the correction results of short-term wind speed forecasts of wind farms. The formula for calculating the error index is as follows:

$$R = \frac{\sum_{i}^{n}\left(y_i - \bar{y}\right)\left(\hat{y}_i - \bar{\hat{y}}\right)}{\sqrt{\sum_{i=1}^{n}\left(y_i - \bar{y}\right)^2}\sqrt{\sum_{i=1}^{n}\left(\hat{y}_i - \bar{\hat{y}}\right)^2}} \quad (1.9)$$

$$RMSE = \sqrt{\frac{1}{n}\sum_{i=1}^{n}\left(\hat{y}_i - y_i\right)^2} \quad (1.10)$$

$$MAE = \frac{1}{n}\sum_{i=1}^{n}\left|\hat{y}_i - y_i\right| \quad (1.11)$$

https://doi.org/10.5194/egusphere-2023-945
Preprint. Discussion started: 31 May 2023

$$rRMSE = \left[\sqrt{\frac{1}{n}\sum_{i=1}^{n}(\hat{y}_i - y_i)^2} \Big/ \left(\frac{1}{n}\sum_{i=1}^{n} y_i \right) \right] \times 100\% \tag{1.12}$$

$$rMAE = \left(\frac{1}{n}\sum_{i=1}^{n}\left|\hat{y}_i - y_i\right| \Big/ \left(\frac{1}{n}\sum_{i=1}^{n} y_i \right) \right) \times 100\% \tag{1.13}$$

$$FA = N_r / N_f \tag{1.14}$$

Among them, n represents the number of samples, $\hat{y}_i$ represents the i-th predicted value, y_i represents the i-th actual value; N_r represents the number of wind speed absolute errors not greater than 1 m/s, and N_f represents the number of research samples.

3 Results

3.1 Experiment 1 evaluation

In Experiment 1, the BOA optimization algorithm was applied to five AI models to correct the 10-meter wind speed forecasted by WRF. There were 12 meteorological element features to establish five different AI models (see Table 2 for the hyper-parameters of the five AI models). The training, validation, and testing results for 10-meter wind speed are shown in Figures S1-5 in the supplementary material. The RMSE values between the predicted and the observed value of the training set (validation set) in the lightGBM, XGBoost, RF, DBN, and MLP models are 0.41 m/s (0.54 m/s), 0.31 m/s (0.56 m/s), 0.52 m/s (0.57 m/s), 0.59 m/s (0.62 m/s) and 0.73 m/s (0.73 m/s). The FA are 0.98 (0.94), 0.99 (0.93), 0.94 (0.93), 0.92 (0.91), and 0.88 (0.88). The R squared are 0.87 (0.77), 0.92 (0.75), 0.79 (0.73), 0.72 (0.69), and 0.57 (0.57). It is evident that all models, except the DBN model, can fit the training set data well. The DBN model exhibits the weakest performance on both the training and validation sets. Alternatively, the LightGBM and XGBoost models demonstrate superior prediction performance on the training set compared to the validation set. The scatter points of the training sets of these two models accumulate on the 1:1 diagonal, indicating slight overfitting. The RMSE of lightGBM, XGBoost, RF, DBN, and MLP models on the test set in December 2021 (January 2022) are 0.67 m/s (0.64 m/s), 0.70 m/s (0.67 m/s), 0.65 m/s (0.64 m/s), 0.77 m/s (0.74 m/s), and 0.74 m/s (0.68 m/s) respectively. The FA of models on the test set in December 2021 (January 2022) are 89.68 % (91.11 %), 87.90 % (89.88 %), 90.64 % (91.36 %), 86.74 % (87.71 %), and 86.08 % (89.57 %). The R are 0.79 (0.77), 0.77 (0.75), 0.81 (0.78), 0.71 (0.68), and 0.75 (0.74). Considering different evaluation indexes, the revision effects of the five models in two months demonstrate that RMSE is that January 2022 is generally lower than December 2021; FA is that January 2022 is generally higher than December 2021; R is that January 2022 is generally lower than December 2021. Overall, the prediction performance of the five models in January 2022 surpassed that in December 2021. Furthermore, the LightGBM and RF models exhibited the best performance among the five models in the two-month test sets, while the DBN model had the least effective correction effect.

With respect to the importance of RF characteristics (Fig.6a, c), it is indisputable that the 10 m wind speed predicted by WRF plays a dominant role in correcting the actual wind speed. The ones following are latitude, longitude and topographic height, which represent spatial geographic information, and the actual wind speed is closely related to geographic information. Subsequently, relative humidity is of lesser importance. The distribution of the humidity field typically correlates with the movement of the atmosphere, which is also closely related to wind speed. Certain meteorological elements, such as rainfall, 2 m dew-point temperature, and 2 m temperature, contribute less importance.

Table 2. The best hyper-parameters of the models

Model	parameters
VMD-PCA-lightGBM	‘max_depth’ : 28, ‘min_child_samples’ : 30, ‘n_estimators’ : 436, ‘num_leaves’ : 287
VMD-PCA-XGBoost	‘gamma’ : 1, ‘max_depth’ : 19, ‘min_child_weight’ : 1, ‘n_estimators’: 408
VMD-PCA-RF	‘max_depth’ : 31, ‘max_features’ : 14, ‘min_samples_leaf’ : 28, ‘min_samples_split’ : 3, ‘n_estimators’ : 371
VMD-PCA-DBN	‘input_length’ : 20, ’output_length’ : 1, ’loss_function’ : ‘MSE’, ’optimizer’ : ‘Adam’, ’hidden_units’ : [400, 200], ’batch_size’ :20000, ’epoch_pretrain’ : 100, ’epoch_finetune’ : 200
VMD-PCA-MLP	‘batch_size’ : 10114, ‘hidden_layer_sizes’ : 305, ‘max_iter’ : 386
lightGBM	‘max_depth’ : 21, ‘min_child_samples’ : 19, ‘n_estimators’ : 312, ‘num_leaves’ : 297

https://doi.org/10.5194/egusphere-2023-945
Preprint. Discussion started: 31 May 2023

XGBoost	'gamma' : 0, 'max_depth' : 21, 'min_child_weight' : 9, 'n_estimators': 299
RF	'max_depth' : 40, 'max_features' : 12, 'min_samples_leaf' : 23, 'min_samples_split' : 2, 'n_estimators' : 440
DBN	'input_length' : 12, 'output_length' : 1, 'loss_function' : 'MSE', 'optimizer' : 'Adam', 'hidden_units' : [400, 200], 'batch_size' : 20000, 'epoch_pretrain' : 100, 'epoch_finetune' : 200
MLP	'batch_size' : 10232, 'hidden_layer_sizes' : 494, 'max_iter' : 311

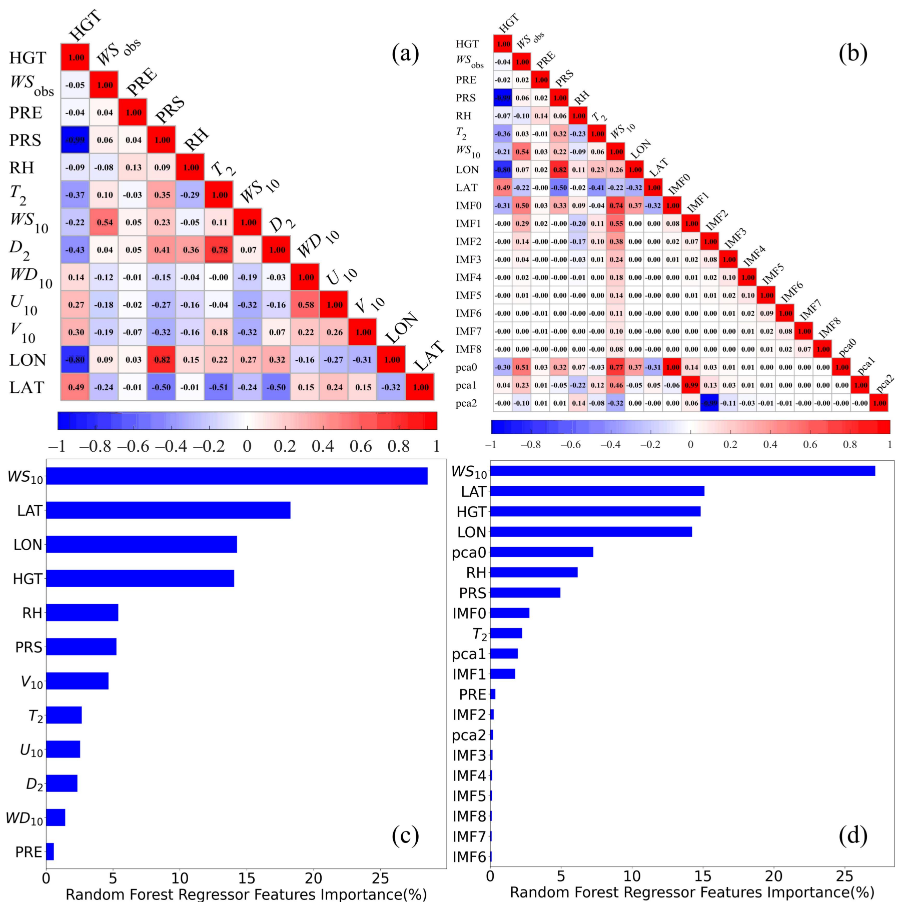

Figure 6: Schematic diagram of correlation and feature importance for two sets of experiments. (a) and (c) represent experiment 1, and (b) and (d) represent experiment 2.

https://doi.org/10.5194/egusphere-2023-945
Preprint. Discussion started: 31 May 2023

3.2 Experiment 2 evaluation

Experiment 2 builds upon Experiment 1, concentrating on the predicted 10-meter wind speed by the WRF model. We use the VMD algorithm to decompose the predicted wind speed into 9 components, and use the PCA algorithm to extract the main 3 principal components. In the RF feature importance analysis (Fig.6b, d), it is evident the VMD algorithm can decompose IMF0 and IMF1, with contributions surpassing those of 2-meter temperature and precipitation, respectively. The importance of the pca0 component, after PCA principal component extraction, reaches up to 8%. What is particularly interesting is that in the correlation analysis, the correlation values between the IMF0 and pca0 components and the actual wind speed are 0.50 and 0.51, which are second only to the forecasted wind speed.

The RMSE between the predicted value and the observed value of the training set (validation set) in the VMD-PCA-lightGBM, VMD-PCA-XGBoost, VMD-PCA-RF, VMD-PCA-DBN, and VMD-PCA-MLP models are 0.33 m/s (0.53 m/s), 0.31 m/s (0.54 m/s), 0.52 m/s (0.57 m/s), 0.75 m/s (0.75 m/s) and 0.60 m/s (0.66 m/s). The FA are 0.99 (0.94), 1.00 (0.94), 0.94 (0.93), 0.87 (0.87), and 0.91 (0.90). The R squared are 0.91 (0.77), 0.93 (0.77), 0.79 (0.73), 0.55 (0.55), and 0.71 (0.65). These are shown in supplementary materials Figures S6-8. In comparison to the above five artificial intelligence methods, training results of VMD-PCA-DBN are relatively inferior. VMD-PCA-lightGBM and VMD-PCA-XGBoost models still train the processed data effectively. According to the scatter density figure (Fig.7a, Fig.8a), the scatter points are relatively concentrated on the 1:1 line. The RMSE of VMD-PCA-lightGBM, VMD-PCA-XGBoost, VMD-PCA-RF, VMD-PCA-DBN, and VMD-PCA-MLP models on the test set in December 2021 (January 2022) are 0.63 m/s (0.63 m/s), 0.68 m/s (0.66 m/s), 0.62 m/s (0.64 m/s), 0.77 m/s (0.76 m/s), and 0.71 m/s (0.69 m/s) respectively. The FA of the five models on the test set in December 2021 (January 2022) are 91.13 % (91.49 %), 89.22 % (90.23 %), 91.79 % (91.57 %), 87.93 % (87.61 %), and 87.20 % (88.94 %). The R are 0.81 (0.78), 0.78 (0.76), 0.82 (0.78), 0.71 (0.67), and 0.75 (0.73). The test results of the five models in Experiment 2 in December 2021 and January 2022 show that the error indexes of RMSE and FA of each model exhibit minimal difference in two months. Nonetheless, disregarding the correlation coefficient (R) results, the performance of the five models in December 2021 is inferior to that in January 2022. The diurnal variation scatter plot of two months is tested. The red scatter represents the

https://doi.org/10.5194/egusphere-2023-945
Preprint. Discussion started: 31 May 2023

nighttime wind speed, which is more concentrated on the 1:1 line. In contrast, the blue scatter represents the afternoon wind speed, which is slightly away from the 1:1 line. This suggests that the correction effect of the five models exhibits a noticeable diurnal variation.

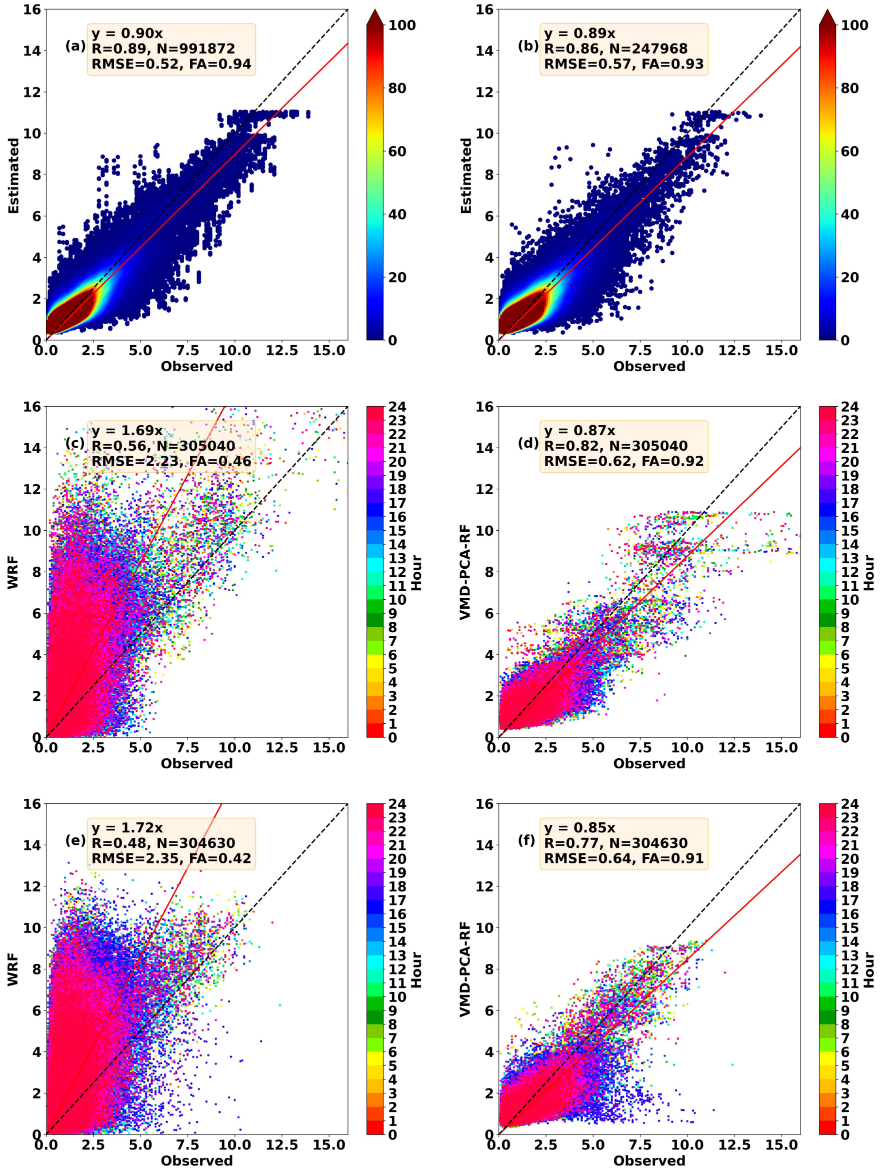

Figure 7: The 24-hour scatter density map compared with the actual 10-meter wind speed. (a) 10-fold cross-validation training set of VMD-PCA-RF model in February 2022, (b) 10-fold cross-validation validation set of VMD-PCA-RF model in February 2022, (c) WRF forecasts in December 2021, (d)

https://doi.org/10.5194/egusphere-2023-945
Preprint. Discussion started: 31 May 2023

VMD-PCA-RF model forecasts in December 2021, (e) WRF forecasts in January 2022, and (f) VMD-PCA-RF model forecasts in January 2022.

https://doi.org/10.5194/egusphere-2023-945
Preprint. Discussion started: 31 May 2023

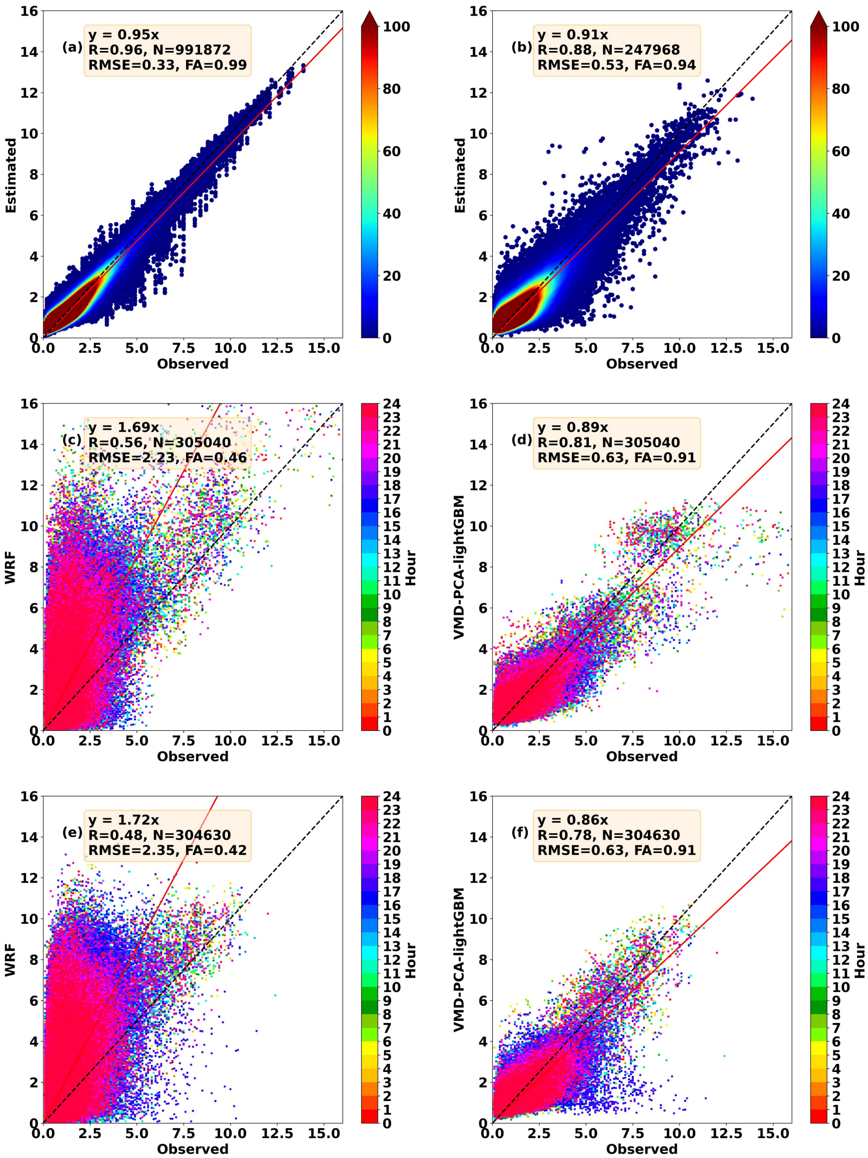

Figure 8: The 24-hour scatter density map compared with the actual 10-meter wind speed. (a) 10-fold cross-validation training set of VMD-PCA-lightGBM model in February 2022, (b) 10-fold cross-validation validation set of VMD-PCA- lightGBM model in February 2022, (c) WRF forecasts in December 2021, (d) VMD-PCA- lightGBM model forecasts in December 2021, (e) WRF forecasts in January 2022, (f) VMD-PCA- lightGBM model forecasts in January 2022.

https://doi.org/10.5194/egusphere-2023-945
Preprint. Discussion started: 31 May 2023

3.3 Comparison of the two experiments

Firstly, all 10 models effectively corrected the 10-meter wind speed forecasted by WRF. Table 3 and Table 4 represent the evaluation indexes of wind speed errors predicted by 10 models in December 2021 and January 2022. From the two tables, it is evident that the VMD-PCA-RF and VMD-PCA-lightGBM models have the best performance in December 2021 and January 2022, respectively, with the most comprehensive performance of the forecast indicators. The MAE, RMSE, rMAE, rMAE, and FA for the two models VMD-PCA-RF (VMD-PCA-lightGBM) were 0.46 m/s (0.45 m/s), 0.62 m/s (0.63 m/s), 37.36 % (34.75 %), 50.39 % (48.65 %), and 91.79 % (91.49 %) in December 2021 (January 2022). Additionally, based on the analysis of the Taylor chart (Fig.9e, f) of 10 models in Fig.9, it can also be seen that the scatter distance of VMD-PCA-RF and VMD-PCA-lightGBM models is closest to the observed black dotted line and the black triangle position. The two models show that the standard deviation is close to the observed wind speed, with the lowest RMSE and the highest R. Secondly, in the comparison of cumulative probability distributions, all models passed Kolmogorov's 5 % confidence interval test when the interval of wind speed is 0.5 m/s (Fig.9a, d). However, when the interval of wind speed is 0.2 m/s (Fig.9b, e), VMD-PCA-lightGBM model deviated from Kolmogorov's 5 % confidence interval detection in December 2021. This indicates that the VMD-PCA-RF model has a better predictive effect than VMD-PCA-lightGBM model in December 2021 when the actual wind speed is within the range of 0.4 m/s-0.8 m/s.

Table 3. Table of evaluation indexes of wind speed error predicted by 10 models in December 2021

Model	MAE（m/s）	RMSE（m/s）	rMAE（%）	rRMSE（%）	FA（%）	R
VMD-PCA-lightGBM	0.47	0.63	37.67	51.25	91.13	0.81
VMD-PCA-XGBoost	0.49	0.68	39.84	54.82	89.22	0.78
VMD-PCA-RF	0.46	0.62	37.36	50.39	91.79	0.82
VMD-PCA-DBN	0.53	0.75	43.32	61.13	87.93	0.71
VMD-PCA-MLP	0.53	0.72	43.04	58.47	87.2	0.75
lightGBM	0.49	0.67	39.59	54.16	89.68	0.79
XGBoost	0.51	0.70	41.51	56.64	87.9	0.77
RF	0.48	0.65	38.80	52.32	90.64	0.81
DBN	0.56	0.77	45.25	62.46	86.74	0.71

https://doi.org/10.5194/egusphere-2023-945
Preprint. Discussion started: 31 May 2023

MLP	0.55	0.74	44.65	60.1	86.08	0.75

Table 4. Table of evaluation indexes of wind speed error predicted by 10 models in January 2022

Model	MAE（m/s）	RMSE（m/s）	rMAE（%）	rRMSE（%）	FA（%）	R
VMD-PCA-lightGBM	0.45	0.63	34.75	48.65	91.49	0.78
VMD-PCA-XGBoost	0.47	0.66	36.31	51.01	90.23	0.76
VMD-PCA-RF	0.46	0.64	35.06	49.00	91.57	0.78
VMD-PCA-DBN	0.53	0.75	40.96	57.49	87.61	0.67
VMD-PCA-MLP	0.50	0.69	38.46	53.16	88.94	0.73
lightGBM	0.46	0.64	35.24	49.34	91.11	0.77
XGBoost	0.48	0.67	36.68	51.38	89.88	0.75
RF	0.46	0.64	35.18	49.13	91.36	0.78
DBN	0.53	0.74	40.97	56.86	87.71	0.68
MLP	0.49	0.68	37.83	52.26	89.57	0.74

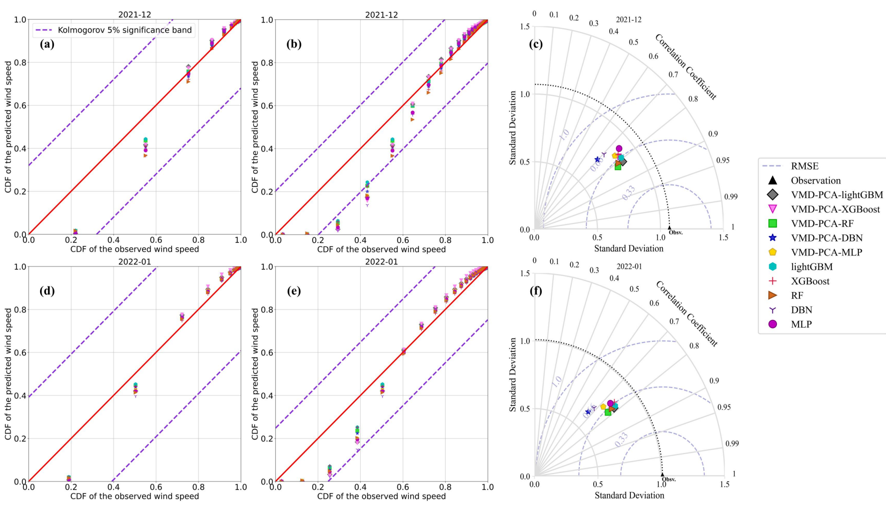

Figure 9: The cumulative distribution probability scatter plots of the actual wind speed and the predicted wind speed of 10 models in wind speed intervals of 0.5 m/s ((a) represents December 2021, (d) represents January 2022) and 0.2 m/s ((b) represents December 2021, (e) represents January 2022) respectively; Taylor distribution map ((c) represents December 2021, (f) represents January 2022).

https://doi.org/10.5194/egusphere-2023-945
Preprint. Discussion started: 31 May 2023

3.4 Spatial–temporal variations in the best models

Based on our comparative analysis results, we conclude that the best performing combination models in December 2021 and January 2022 are VMD-PCA-RF and VMD-PCA-lightGBM respectively. Figure 10 shows the diurnal variation corrections of the two best models for a given month, as well as the diurnal variation of wind speed in the original WRF forecast. The wind speed of the original WRF numerical weather forecast shows noticeable overestimation, which is confirmed in Fig.8c and 8e. The scatter points of WRF forecast predominantly deviate towards the upper left corner, with relatively low correlation coefficients, 0.56 and 0.23, respectively. Furthermore, the wind speed forecast by WRF displays obvious diurnal variation traits, characterized by large errors between afternoon and evening, specifically between 11:00 and 20:00 (Fig.10a, b). Moreover, the actual average wind speed in January 2022 deviates from the range of one standard deviation of the WRF forecast wind speed at 17:00 and 18:00. This demonstrates that the wind speed forecast by WRF is inaccurate and exhibits substantial diurnal variation errors.

After the best model was corrected, the error of diurnal variation is significantly reduced (Fig.10c, d). First, the average wind speed corrected by the best model is essentially consistent with the actual average wind speed curve, with minimal error and no diurnal variation. Second, the one standard deviation range of the corrected and actual wind speeds is also well-matched, indicating that the corrected and actual wind speed distributions are consistent. The correction effect at 16:00 and 17:00 on January 2022 is suboptimal, which may be due to the insufficient generalization of the training model and the excessive fluctuation of the actual wind speed at these two time points.

The FA (Fig.11a, b) and RMSE (Fig.11e, f) distribution of WRF forecast 10-meter wind speed at 410 stations in the five southern provinces shows that the 10-meter wind speed prediction effect of the WRF model in Yunnan is superior to that in the other four provinces. In the Yunnan area, the FA of most WRF forecast station 10-meter wind speeds exceeds 40 %, and RMSE value is mostly below 2.4 m/s. Conversely, in other regions, such as Guangxi, Guangdong and Hainan, the terrain is relatively flat. The FA of the 10-meter wind speed forecast by WRF is as low as 30 % at some stations, and the RMSE reaches up to 5.4 m/s. However, after the VMD-PCA-RF and VMD-PCA-lightGBM models are corrected, the FA of most stations in the five southern provinces is as high as 90 %, and the RMSE is as low as 0.6 m/s. Moreover, in Guangxi, Guangdong, and Hainan, where the WRF forecast effect is

https://doi.org/10.5194/egusphere-2023-945
Preprint. Discussion started: 31 May 2023

subpar, the accuracy of the corrected 10-meter wind speed by VMD-PCA-RF (VMD-PCA-lightGBM) is significantly improved.

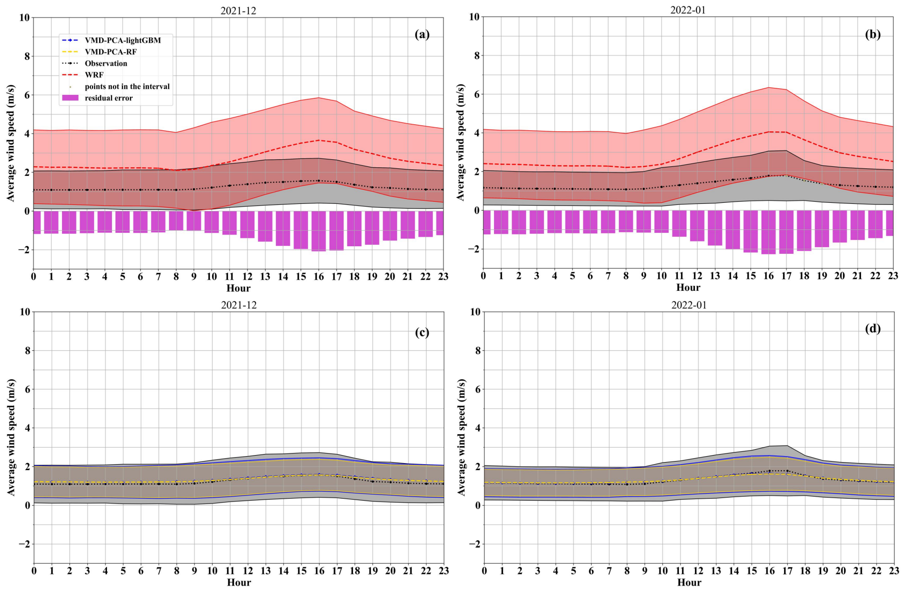

Figure 10: VMD-PCA-lightGBM,VMD-PCA-RF and WRF daily variation of predicted and actual wind speeds in December 2021 and January 2022.

https://doi.org/10.5194/egusphere-2023-945
Preprint. Discussion started: 31 May 2023

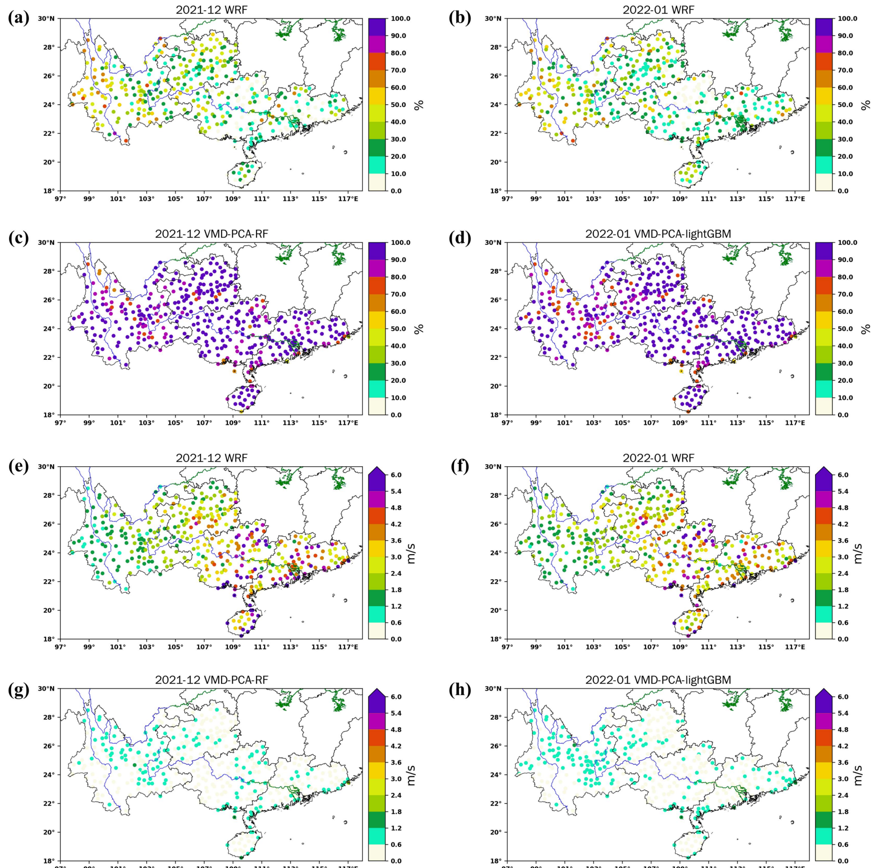

Figure 11: FA and RMSE distribution maps of VMD-PCA-RF, VMD-PCA-lightGBM and WRF models on 410 sites in five southern provinces ((a), (c), (e), and (g) represent December 2021; (b), (d), (f), and (h) represent January 2022).

4. Discussion

4.1 The effects of BOA-VMD-PCA

It is shown in Table 2 that the hyper-parameters of the 10 models in the two experiments are different. Since the DBN model is not added to the scikit-learn Python learning package, it is challenging to call the BOA algorithm for tuning parameters. Apart from the DBN model, all the other models are optimized using the BOA algorithm. From the various evaluation indicators in Table 3 and Table 4, the DBN model, which does not use the BOA algorithm to adjust the model parameters to obtain an optimal parameter configuration, yields the worst prediction results in December 2021 and January 2022. Moreover, studies (Xiong et al., 2022) also have shown that BOA can further improve the model's prediction accuracy by configuring optimal hyper-parameters. The hyper-parameters such as the number of neurons and learning rate in the hidden layer, significantly impact the model's performance. When the same model is applied to different data sets of two experiments, the BOA adaptively obtains the optimal combination of hyper-parameters, overcoming the limitations of manual parameter adjustment (Guo et al., 2021). This suggests that the selection of model hyper-parameters introduces considerable uncertainty into our prediction results. Therefore, the choice of optimization model parameters represents one source of uncertainty in the correction results, which entails the complexity of parameter selection. However, a more advanced parameter tuning method, such as the BOA tuning algorithm, is essential.

The VMD is used to obtain unknown but meaningful features hidden in the 10-meter wind speed sequences predicted using WRF models (Li et al., 2022). In addition, the PCA can extract important components of anemometer subsequences. When the stationary subsequence serves as an input to the error correction model, it contains more valuable information than the previous non-stationary wind speed sequences (Xu et al., 2021).

The complexity of the input factors in this study is one of the sources of uncertainty in the process of correcting WRF prediction results. The input factors of the two experiments are not identical. In the second set of experiments, the input of meteorological factors is reduced based on the first set of experiments, while component information of the 10-meter wind speed predicted by WRF is increased. Multiple wind speed components processed by VMD-PCA and noise reduction are introduced. Among them, the importance of pca0 and IMF0 introduced is approximately 5 %. In the 10-month test sets, the correction accuracy of experiment 2 is no less than the results of experiment 1 (Fig.14, Fig.S9, 10), indicating that the 10-meter wind speed components introduced by the VMD-PCA contribute positively to the correction results.

4.2 RF feature importance

In order to further understand the feature importance ranking of the RF models, we divided the model prediction results and actual wind speeds of the 410 stations into 20 equal parts according to

https://doi.org/10.5194/egusphere-2023-945
Preprint. Discussion started: 31 May 2023

height (Fig.12). First of all, the actual wind speed in December 2021 and January 2022 varies with the height of the station, showing that the lower the height of the station, the more significant the change of wind speed. This relationship is associated with the wind speed profile of the atmosphere, where wind speed increases as height decreases. Secondly, the wind speed during the day is generally greater than the wind speed at night, which is related to the turbulent motion of the atmosphere during the day. Solar radiation causes the atmosphere to mix, resulting in convective movement. The 10-meter wind speed at night is affected by the cooling radiation of the surface, and the atmosphere is relatively stable.

The 10-meter wind speed predicted by WRF has the highest feature importance in the correction process of the RF models. Input factors with distinct geographic information, such as latitude, longitude, and height, rank highly in feature importance. Similarly, when Sun et al. 2019 used machine learning to correct the 10-meter wind speed predicted by the numerical weather prediction model ECMWF, the characteristic weight of the 10-meter wind speed predicted by the model is the highest, followed by the sea-land factor. Also, as the 10-meter wind speed forecast by WRF increases, the instability of the 10-meter wind speed corrected by the 10 machine learning models gradually increased, and the correction accuracy gradually decreased (Fig.13). This partly explains the higher importance of the 10-meter wind speed forecast by WRF.

With 1 km as the center, the measured 10-meter wind speed is more unstable in areas where the station height increases or decreases. However, the 10-meter wind speed predicted by WRF being more unstable with the station height decreases (Fig.12). The VMD-PCA-RF and VMD-PCA-lightGBM models significantly reduce the instability of the 10-meter wind speed predicted by WRF. When the height of the station increases or decreases at 1 km, the correction intensity tends to increase gradually. This further explains the higher importance of the height factor in the RF model training.

https://doi.org/10.5194/egusphere-2023-945
Preprint. Discussion started: 31 May 2023

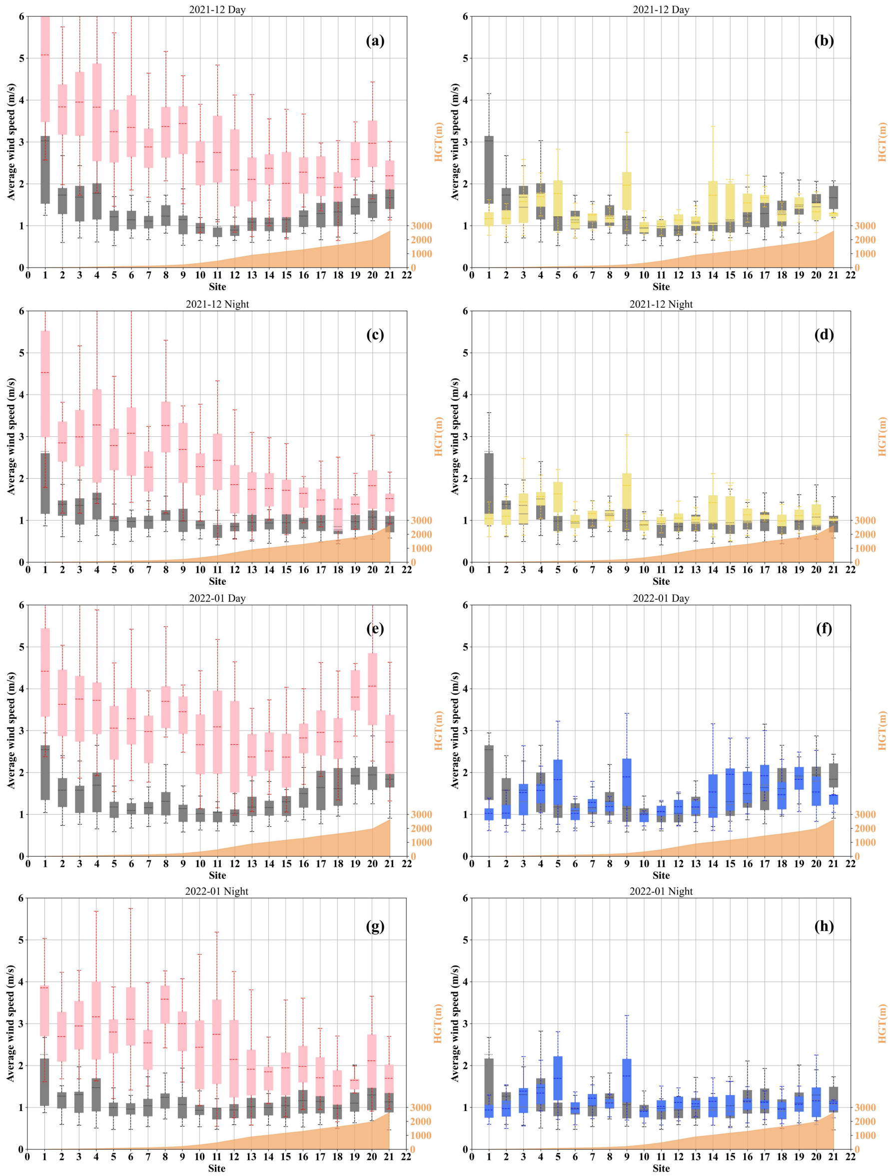

Figure 12: The boxplots of the predicted wind speeds of the VMD-PCA-RF (yellow), VMD-PCA-lightGBM (blue), and WRF (pink) models at 20 stations at different height intervals, and the boxplots of the actual wind speeds (gray).

https://doi.org/10.5194/egusphere-2023-945
Preprint. Discussion started: 31 May 2023

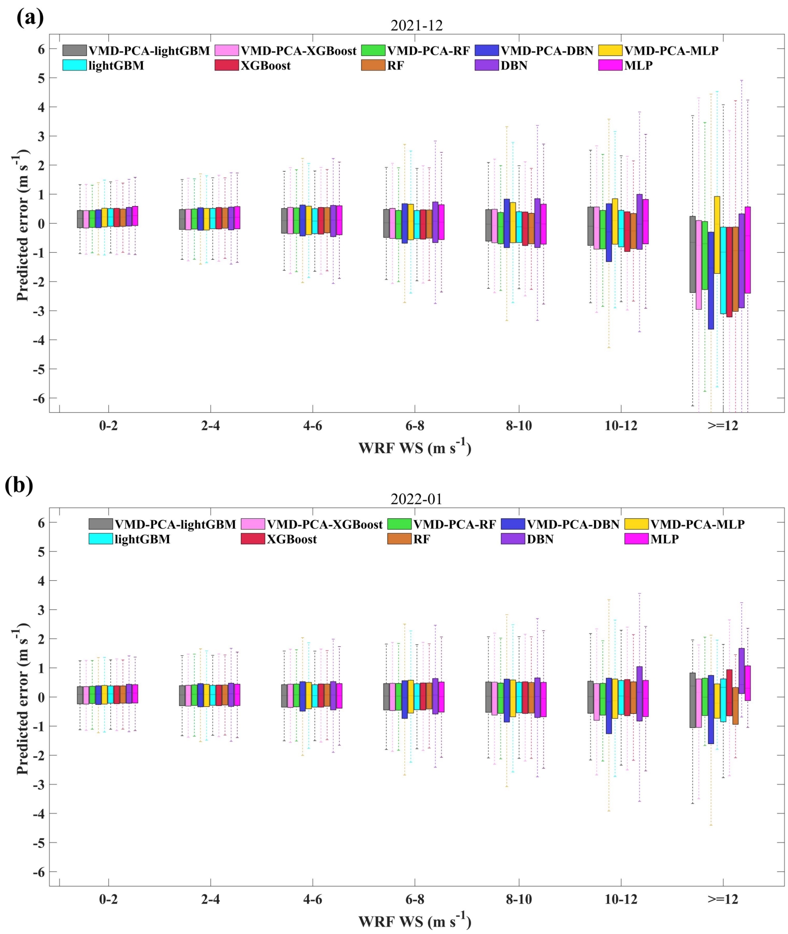

Figure 13: The prediction error boxplots of 10 models in different WRF prediction intervals.

4.3 Stability analysis of the proposed models

In order to identify the best model of the five southern provinces and assess the model's stability, we evaluated all 10 models over 10 different months. Fig.14 shows the evaluation histogram of the 10-meter wind speed predicted by the 10 models in Experiment 1 and Experiment 2, as well as the actual wind speed in various months. Meanwhile, Fig.S9 and S10 can more effectively illustrate the daily changes of the revised results of 10 models in 10 different months. As shown in the figure 14, the evaluation indexes of the model trained in Experiment 2, after VMD-PCA processing, outperform those of the model trained in Experiment 1. The RF model demonstrates exceptional robustness, while

https://doi.org/10.5194/egusphere-2023-945
Preprint. Discussion started: 31 May 2023

the MLP model exhibits the poorest performance. VMD-PCA-RF evaluation indexes are relatively stable across the 10 months, with a correlation coefficient R above 0.6, accuracy rate FA above 85 %, MAE below 0.6 m/s, RMSE below 0.8 m/s, rMAE below 60 %, and rRMSE below 75 %. However, the robustness of the VMD-PCA-lightGBM and VMD-PCA-XGBoost models is inferior to that of the VMD-PCA-RF, with all six evaluation indexes performing worse than the VMD-PCA-RF as the seasons and months change. In general, VMD-PCA-RF is the best wind speed correction model for winter and even throughout the entire year in the five southern provinces.

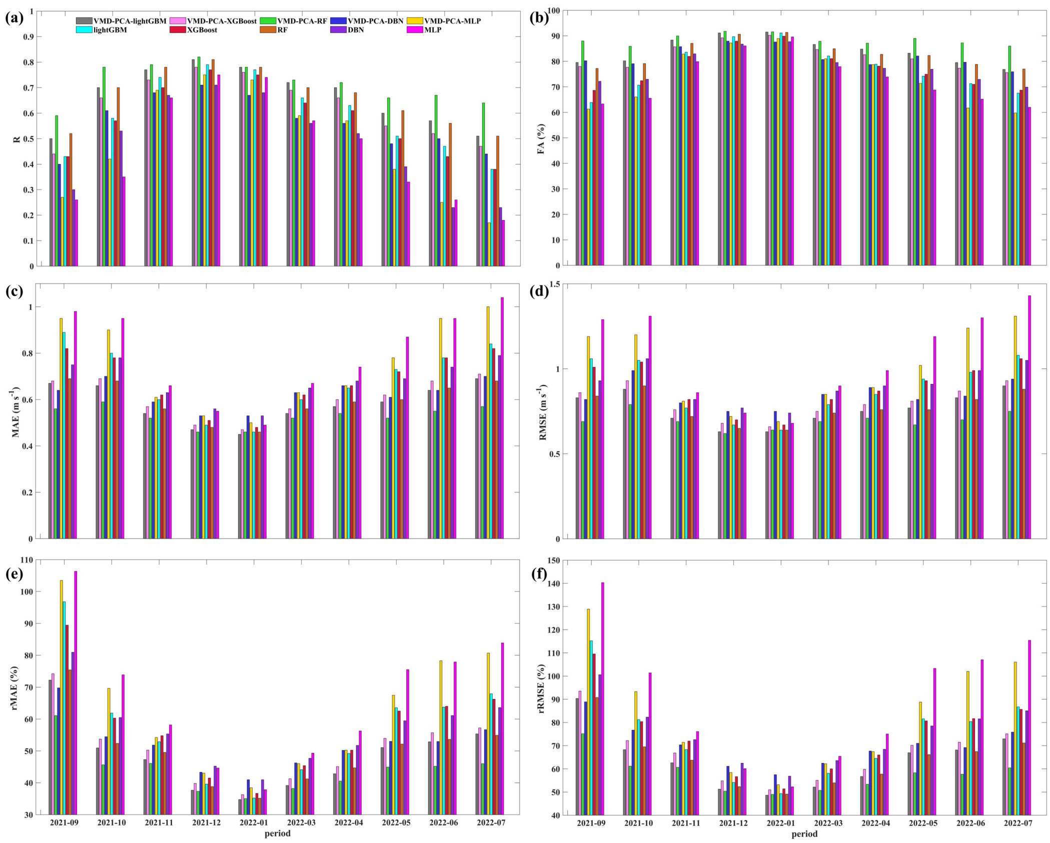

Figure 14: Evaluation histograms of 10-meter wind speed predicted by 10 models and actual wind speed in different months in Experiment 1 and Experiment 2 ((a), (b), (c), (d), (e), and (f) represent R, FA (%), MAE (m/s), RMSE (m/s), rMAE (%), and rRMSE (%) respectively).

https://doi.org/10.5194/egusphere-2023-945
Preprint. Discussion started: 31 May 2023

5. Conclusions

In an effort to enhance the wind speed prediction performance for wind farms, this study developed a WRF-based multi-step wind speed prediction model. A hybrid error correction strategy combining BOA, VMD, PCA, and RF (LightGBM) is proposed to increase the accuracy of WRF simulations. The first group of experiments used various meteorological elements as input factors in a control experiment. In the second group of experiments, the wind speed sequence predicted by the WRF model was decomposed into multiple IMFs using the VMD algorithm for feature extraction. A principal component analysis method is used to extract meaningful principal components from these subsequence IMFs to improve computational efficiency. In the error correction model, RF (lightGBM) and other algorithms are used to train the relationship between different input factors and the actual wind speed error, respectively.

Through a case analysis of 410 stations in five southern provinces in China, the following conclusions can be drawn: (1) The machine learning models tuned by the BOA-VMD-PCA algorithm exhibit a positive impact on wind speed error correction; (2) Feature importance analysis revealed that the top eight contributing factors for correcting WRF forecasted wind speed include WRF forecast 10-meter wind speed (WS10), latitude, longitude, altitude, pca0, humidity, pressure, IMF0; (3) VMD-PCA-RF and VMD-PCA-lightGBM are the most suitable wind speed correction algorithms for December 2021 and January 2022, respectively. The MAE, RMSE, FA, rMAE, rRMSE, and R of the corrected wind speed and the actual wind speed are 0.46 (0.45), 0.62 m/s (0.63 m/s), 37.36 % (34.75 %), 50.39 % (48.65 %), 91.79 % (91.49 %), and 0.82 (0.78); and (4) The proposed wind speed correction model (VMD-PCA-RF) demonstrates the highest prediction accuracy and stability in the five southern provinces in nearly a year and at different heights. VMD-PCA-RF evaluation indexes for 10 months remain relatively stable: correlation coefficient R is above 0.6, accuracy rate FA is above 85 %, MAE is below 0.6 m/s, RMSE is below 0.8 m/s, rMAE is below 60 %, and rRMSE is below 75 %. In future research, the proposed VMD-PCA-RF algorithm can be extrapolated to the 3 km grid points of the five southern provinces to generate a 3km grid-corrected wind speed product.

Code availability

The code and model are available as a free-access repository on Zenodo at https://doi.org/10.5281/zenodo.7940686 (Zhou, 2023).

Data Availability

The data is available as a free-access repository on Zenodo at https://doi.org/10.5281/zenodo.7940686 (Zhou, 2023).

Author contributions

SZ developed the software, visualized the data, and prepared the original draft. SZ and YG developed the methodology and carried out the formal analysis. XX and SZ validated data. SZ, YG, XX, ZD, and YL reviewed and edited the text. All authors have read and agreed to the published version of the paper.

Competing interests

The authors declare that they have no conflict of interest.

Financial support

This research has been supported by the second batch of service public bidding projects for EHV transmission companies in 2022 (2022-FW-2-ZB) (grant no. CG0100022001526556).

https://doi.org/10.5194/egusphere-2023-945
Preprint. Discussion started: 31 May 2023

References

Barthelmie, R. J., Palutikof, J. P., and Davies, T. D.: Estimation of sector roughness lengths and the effect on prediction of the vertical wind speed profile, Boundary-Layer Meteorol, 66, 19–47, https://doi.org/10.1007/BF00705458, 1993.

Cassola, F. and Burlando, M.: Wind speed and wind energy forecast through Kalman filtering of Numerical Weather Prediction model output, Applied Energy, 99, 154–166, https://doi.org/10.1016/j.apenergy.2012.03.054, 2012.

Chen, K. and Yu, J.: Short-term wind speed prediction using an unscented Kalman filter based state-space support vector regression approach, Applied Energy, 113, 690–705, https://doi.org/10.1016/j.apenergy.2013.08.025, 2014.

Cheng, W. Y. Y., Liu, Y., Liu, Y., Zhang, Y., Mahoney, W. P., and Warner, T. T.: The impact of model physics on numerical wind forecasts, Renewable Energy, 55, 347–356, https://doi.org/10.1016/j.renene.2012.12.041, 2013.

Deng, Y., Wang, B., and Lu, Z.: A hybrid model based on data preprocessing strategy and error correction system for wind speed forecasting, Energy Conversion and Management, 212, 112779, https://doi.org/10.1016/j.enconman.2020.112779, 2020.

Dhiman, H. S. and Deb, D.: A Review of Wind Speed and Wind Power Forecasting Techniques, arXiv:2009.02279 [cs, eess], 2020.

Dong, L., Ren, L., Gao, S., Gao, Y., and Liao, X.: Studies on wind farms ultra-short term NWP wind speed correction methods, in: 2013 25th Chinese Control and Decision Conference (CCDC), 2013 25th Chinese Control and Decision Conference (CCDC), Guiyang, China, 1576–1579, https://doi.org/10.1109/CCDC.2013.6561180, 2013.

Erdem, E. and Shi, J.: ARMA based approaches for forecasting the tuple of wind speed and direction, Applied Energy, 88, 1405–1414, https://doi.org/10.1016/j.apenergy.2010.10.031, 2011.

Guo, X., Zhu, C., Hao, J., Zhang, S., and Zhu, L.: A hybrid method for short-term wind speed forecasting based on Bayesian optimization and error correction, Journal of Renewable and Sustainable Energy, 13, 036101, https://doi.org/10.1063/5.0048686, 2021.

https://doi.org/10.5194/egusphere-2023-945
Preprint. Discussion started: 31 May 2023

Guo, Z., Zhao, W., Lu, H., and Wang, J.: Multi-step forecasting for wind speed using a modified EMD-based artificial neural network model, Renewable Energy, 37, 241–249, https://doi.org/10.1016/j.renene.2011.06.023, 2012.

Hanifi, S., Liu, X., Lin, Z., and Lotfian, S.: A Critical Review of Wind Power Forecasting Methods—Past, Present and Future, Energies, 13, 3764, https://doi.org/10.3390/en13153764, 2020.

Hu, H., Wang, L., and Tao, R.: Wind speed forecasting based on variational mode decomposition and improved echo state network, Renewable Energy, 164, 729–751, https://doi.org/10.1016/j.renene.2020.09.109, 2021.

Hu, J., Wang, J., and Zeng, G.: A hybrid forecasting approach applied to wind speed time series, Renewable Energy, 60, 185–194, https://doi.org/10.1016/j.renene.2013.05.012, 2013.

Huang, Y., Yang, L., Liu, S., and Wang, G.: Multi-Step Wind Speed Forecasting Based On Ensemble Empirical Mode Decomposition, Long Short Term Memory Network and Error Correction Strategy, Energies, 12, 1822, https://doi.org/10.3390/en12101822, 2019.

Isham, M. F., Leong, M. S., Lim, M. H., and Ahmad, Z. A.: Variational mode decomposition: mode determination method for rotating machinery diagnosis, J VIBROENG, 20, 2604–2621, https://doi.org/10.21595/jve.2018.19479, 2018.

James, E. P., Benjamin, S. G., and Marquis, M.: Offshore wind speed estimates from a high-resolution rapidly updating numerical weather prediction model forecast dataset, Wind Energy, 21, 264–284, https://doi.org/10.1002/we.2161, 2018.

Jiménez, P. A. and Dudhia, J.: Improving the Representation of Resolved and Unresolved Topographic Effects on Surface Wind in the WRF Model, Journal of Applied Meteorology and Climatology, 51, 300–316, https://doi.org/10.1175/JAMC-D-11-084.1, 2012.

Joyce, L. and Feng Z.: Global Wind Report 2023, Global Wind Energy Council, https://gwec.net/globalwindreport2023 (last access: 9 May 2023), 2023.

Landberg, L.: Short-term prediction of the power production from wind farms, Journal of Wind Engineering and Industrial Aerodynamics, 80, 207–220, https://doi.org/10.1016/S0167-6105(98)00192-5, 1999.

Li, G. and Shi, J.: Application of Bayesian model averaging in modeling long-term wind speed distributions, Renewable Energy, 35, 1192–1202, https://doi.org/10.1016/j.renene.2009.09.003, 2010.

https://doi.org/10.5194/egusphere-2023-945
Preprint. Discussion started: 31 May 2023

Li, Y., Tang, F., Gao, X., Zhang, T., Qi, J., Xie, J., Li, X., and Guo, Y.: Numerical Weather Prediction Correction Strategy for Short-Term Wind Power Forecasting Based on Bidirectional Gated Recurrent Unit and XGBoost, Front. Energy Res., 9, 836144, https://doi.org/10.3389/fenrg.2021.836144, 2022.

Liu, H., Mi, X., and Li, Y.: An experimental investigation of three new hybrid wind speed forecasting models using multi-decomposing strategy and ELM algorithm, Renewable Energy, 123, 694–705, https://doi.org/10.1016/j.renene.2018.02.092, 2018.

Liu, Y., Wang, Y., Li, L., Han, S., and Infield, D.: Numerical weather prediction wind correction methods and its impact on computational fluid dynamics based wind power forecasting, Journal of Renewable and Sustainable Energy, 8, 033302, https://doi.org/10.1063/1.4950972, 2016.

Ma, Z., Chen, H., Wang, J., Yang, X., Yan, R., Jia, J., and Xu, W.: Application of hybrid model based on double decomposition, error correction and deep learning in short-term wind speed prediction, Energy Conversion and Management, 205, 112345, https://doi.org/10.1016/j.enconman.2019.112345, 2020.

Prósper, M. A., Otero-Casal, C., Fernández, F. C., and Miguez-Macho, G.: Wind power forecasting for a real onshore wind farm on complex terrain using WRF high resolution simulations, Renewable Energy, 135, 674–686, https://doi.org/10.1016/j.renene.2018.12.047, 2019.

Salcedo-Sanz, S., Ángel M. Pérez-Bellido, Ortiz-García, E. G., Portilla-Figueras, A., Prieto, L., and Paredes, D.: Hybridizing the fifth generation mesoscale model with artificial neural networks for short-term wind speed prediction, Renewable Energy, 34, 1451–1457, https://doi.org/10.1016/j.renene.2008.10.017, 2009.

Salcedo-Sanz, S., Ortiz-García, E., Pérez-Bellido, Á., Portilla-Figueras, A., and Prieto, L.: Short term wind speed prediction based on evolutionary support vector regression algorithms, Expert Syst. Appl., 38, 4052–4057, https://doi.org/10.1016/j.eswa.2010.09.067, 2011.

Sun, Q., Jiao, R., Xia, J., Yan, Z., Li, H., Sun, J., Wang, L., and Liang, Z.: Adjusting Wind Speed Prediction of Numerical Weather Forecast Model Based on Machine Learning Methods. Meteorological Monthly, 45(3): 426-436. https://doi.org/10.7519/j.issn.1000-0526.2019.03.012, 2019.

Tang, R., Ning, Y., Li, C., Feng, W., Chen, Y., and Xie, X.: Numerical Forecast Correction of Temperature and Wind Using a Single-Station Single-Time Spatial LightGBM Method, Sensors, 22, 193, https://doi.org/10.3390/s22010193, 2021.

https://doi.org/10.5194/egusphere-2023-945
Preprint. Discussion started: 31 May 2023

Tascikaraoglu, A. and Uzunoglu, M.: A review of combined approaches for prediction of short-term wind speed and power, Renewable and Sustainable Energy Reviews, 34, 243–254, https://doi.org/10.1016/j.rser.2014.03.033, 2014.

Wang, C., Zhang, H., Fan, W., and Ma, P.: A new chaotic time series hybrid prediction method of wind power based on EEMD-SE and full-parameters continued fraction, Energy, 138, 977–990, https://doi.org/10.1016/j.energy.2017.07.112, 2017.

Wang, J. and Hu, J.: A robust combination approach for short-term wind speed forecasting and analysis – Combination of the ARIMA (Autoregressive Integrated Moving Average), ELM (Extreme Learning Machine), SVM (Support Vector Machine) and LSSVM (Least Square SVM) forecasts using a GPR (Gaussian Process Regression) model, Energy, 93, 41–56, https://doi.org/10.1016/j.energy.2015.08.045, 2015.

Williams, J. L., Maxwell, R. M., and Monache, L. D.: Development and verification of a new wind speed forecasting system using an ensemble Kalman filter data assimilation technique in a fully coupled hydrologic and atmospheric model: Data Assimilation in a Coupled Forecasting System, J. Adv. Model. Earth Syst., 5, 785–800, https://doi.org/10.1002/jame.20051, 2013.

Xiong, X., Guo, X., Zeng, P., Zou, R., and Wang, X.: A Short-Term Wind Power Forecast Method via XGBoost Hyper-Parameters Optimization, Front. Energy Res., 10, 905155, https://doi.org/10.3389/fenrg.2022.905155, 2022.

Xu, Q., He, D., Zhang, N., Kang, C., Xia, Q., Bai, J., and Huang, J.: A Short-Term Wind Power Forecasting Approach With Adjustment of Numerical Weather Prediction Input by Data Mining, IEEE Trans. Sustain. Energy, 6, 1283–1291, https://doi.org/10.1109/TSTE.2015.2429586, 2015.

Xu, W., Liu, P., Cheng, L., Zhou, Y., Xia, Q., Gong, Y., and Liu, Y.: Multi-step wind speed prediction by combining a WRF simulation and an error correction strategy, Renewable Energy, 163, 772–782, https://doi.org/10.1016/j.renene.2020.09.032, 2021.

Zhang, D., Peng, X., Pan, K., and Liu, Y.: A novel wind speed forecasting based on hybrid decomposition and online sequential outlier robust extreme learning machine, Energy Conversion and Management, 180, 338–357, https://doi.org/10.1016/j.enconman.2018.10.089, 2019a.

https://doi.org/10.5194/egusphere-2023-945
Preprint. Discussion started: 31 May 2023

Zhang, Y., Chen, B., Pan, G., and Zhao, Y.: A novel hybrid model based on VMD-WT and PCA-BP-RBF neural network for short-term wind speed forecasting, Energy Conversion and Management, 195, 180–197, https://doi.org/10.1016/j.enconman.2019.05.005, 2019b.

Zhang, Z., Ye, L., Qin, H., Liu, Y., Wang, C., Yu, X., Yin, X., and Li, J.: Wind speed prediction method using Shared Weight Long Short-Term Memory Network and Gaussian Process Regression, Applied Energy, 247, 270–284, https://doi.org/10.1016/j.apenergy.2019.04.047, 2019c.

Zhao, J., Guo, Z.-H., Su, Z.-Y., Zhao, Z.-Y., Xiao, X., and Liu, F.: An improved multi-step forecasting model based on WRF ensembles and creative fuzzy systems for wind speed, Applied Energy, 162, 808–826, https://doi.org/10.1016/j.apenergy.2015.10.145, 2016.

Zhao, J., Wang, J., Guo, Z., Guo, Y., Lin, W., and Lin, Y.: Multi-step wind speed forecasting based on numerical simulations and an optimized stochastic ensemble method, Applied Energy, 255, 113833, https://doi.org/10.1016/j.apenergy.2019.113833, 2019.

Zhou, S.: A hybrid method for numerical weather prediction wind speed based on Bayesian optimization (version 1.2.0) and error correction: First release of my code. Zenodo [code] https://doi.org/10.5281/zenodo.7940686, 2023.

Zjavka, L.: Wind speed forecast correction models using polynomial neural networks, Renewable Energy, 83, 998–1006, https://doi.org/10.1016/j.renene.2015.04.054, 2015.